Reduction of crosstalk in blended-shot migration

Jörg Schleicher* (IMECC/UNICAMP & INCT-GP), Jessé C. Costa (FGeo/UFPA & INCT-GP), and Amélia Novais (IMECC/UNICAMP & INCT-GP)

Abstract

When migrating more than one shot at the same time, the nonlinearity of the imaging condition causes the final image to contain the so-called crosstalk, i.e., the results of the interference of wavefields associated with different sources. In this work, we study various ideas of using weights in the image condition, called encoding, for the reduction of crosstalk. We combine the ideas of random phase and/or amplitude encoding and random alteration of the sign with additional multiplication with powers of the imaginary unit. This procedure moves part of the crosstalk to the imaginary part of the resulting image, leaving the desired crosscorrelation in the real part. In this way, the final image is less impaired. Our results indicate that with a combination of these weights, the crosstalk can be reduced by a factor of 4. Moreover, we evaluate the selection procedure of sources contributing to each group of shots. We compare random choice with a deterministic procedure, where the random numbers are exchanged for numbers similar to those of a Costas array. These numbers preserve certain properties of a random choice, but avoid the occurrence of patterns in the distribution. The objective is to avoid that nearby sources can be added to the same group of shots, which cannot be guaranteed with a random choice. Finally, we show that the crosstalk noise can be reduced after migration by image processing.

Introduction

Due to the great effort needed to migrate data from an acquisition consisting of a large number of sources, as required in 3D seismics, blended-shot migration processes data from more than one source simultaneously (Temme, 1984). This idea is based on the observation that the (full or one-way) wave equation is a linear operation, i.e., the wavefield produced by a set of sources is equal to the sum of the wavefields produced by each source acting alone.

The problem with this procedure arises when applying the image condition, conventionally a crosscorrelation between the wavefield propagated down from source and the recorded field, backpropagated from the receivers. When migrating shot groups, we replace the individual fields associated with a single source by a sum over a shot group. The result is a modified image consisting of two contributions, one being the desired image and other the interference from fields associated with different sources, called crosstalk. Thus, this procedure is only feasible in practice, if the crosstalk is considerably smaller than the desired image. Since the number of individual crosstalk contributions is higher than that those to the image, measures must be taken to reduce each of them in comparison to the desired image.

Several ideas on how to achieve the reduction of crosstalk have been discussed in the literature, based on the encoding of the sources, i.e., the inclusion of weights in the image condition. Denoting the source and receiver weights by w_{gk} and $\tilde{w}_{gk}$, the final energy distribution between image and crosstalk depends on the matrix

$$W_{kj} = \sum_{g=1}^{G} w_{gk} \tilde{w}^*_{gj} \; . \tag{1}$$

Ideally, we would like to choose the weights such that $W_{kj} = \delta_{kj}$, with δ_{kj} denoting the Kronecker delta. This would mean no crosstalk. As this cannot be satisfied exactly, we need the best possible approximation.

The work of Romero et al. (2000) contains several proposals for phase encoding (linear, random, by frequency modulation – chirp). However, the noise reduction achieved in that study was not sufficient to allow for the sum of large numbers of sources. Other ideas include the alteration of the sign (Sun et al., 2002), source modulation (Soubaras, 2006), phase encoding using gold codes (Guerra and Biondi, 2008), random amplitude encoding (Godwin and Sava, 2010) and source decimation (Godwin and Sava, 2011).

In this work we combine the ideas of random phase and amplitude encoding and sign alteration with additional multiplication with the weight $w_{gk} = \tilde{w}_{gk} = i^g$. In this way, half the crosstalk passes to the imaginary part of the resulting image, while the desired image is unchanged. Thus, the real part of the modified image is less affected by crosstalk.

Additionally to encoding, we evaluate the influence of the choice of sources contributing to each shot group. We compare the random choice with a procedure, where the random numbers are exchanged for numbers similar to those of a Costas array (Costas, 1965; Golomb and Taylor, 1984; Drakakis and Rickard, 2010). These numbers preserve certain properties of a random choice, but avoid the occurrence of patterns in the distribution. The goal is to avoid that nearby sources can be added to the same shot group, which cannot be guaranteed with a random choice.

Finally, under the hypothesis that the crosstalk behaves like random noise with zero mean, we apply a denoising technique borrowed from image processing to the results of a blended-shot migration.

Weight functions

Random encoding makes use of a random variable to calculate the weights. We have investigated the following weights functions.

- Random phase encoding (between $-\pi$ and π)

$$w_{gj} = \begin{cases} \exp\{i\pi(2r_j - 1)\} & \text{continuous} \\ \exp\{i\pi \frac{2[\![Mr_j]\!] - M + 1}{M-1}\} & M \text{ levels} \end{cases} \quad (2)$$

  and $\tilde{w}_{gj} = w_{gj}$.

- Random amplitude encoding (between -1 and 1)

$$w_{gj} = \begin{cases} 2r_j - 1 & \text{continuous} \\ (2[\![Mr_j]\!] - M + 1)/(M-1) & M \text{ levels.} \end{cases} \quad (3)$$

  Here, we also used $\tilde{w}_{gj} = w_{gj}$, although this choice degrades the quality of image $\hat{I}$. The choice $\tilde{w}_{gj} = 1/w_{gj}$ would avoid this degradation, but introduces instabilities when the weights are very small.

- Random choice of sign (only factors -1 or 1)

$$w_{gj} = \text{sgn}(2r_j - 1) \quad \text{and} \quad \tilde{w}_{gj} = w_{gj} \; . \quad (4)$$

  Note that this choice is a subset of both preceeding ones. It corresponds to a two-level phase or amplitude encoding (phase $-\pi$ and π, or amplitude -1 e 1).

- Deterministic imaginary-unit weight per group

$$w_{gj} = i^g \quad \text{and} \quad \tilde{w}_{gj} = w_{gj} \; . \quad (5)$$

- Combinations of these weights, like the product of weights (2) and (3), (2) and (5), (4) and (5), (2), (3) and (5), etc.

In the above formulas, r_j is the j-th realization of a random variable, uniformly distributed between 0 and 1, and the operator $[\![.]\!]$ denotes the Gauss brackets, defining the largest integer less than its argument.

Group composition

Another question regarding the grouping of shots for the purpose of migration refers to the selection of shots joined into groups. Besides classical choices like the simulation of plane or cylindrical waves, the random choice of shots is suggested in the literature. However, by not controlling the choice, patterns can form that may affect the final image. An example for such patterns would be the choice of neighboring shots showing strong correlations between them. In this paper, we investigate a way to mitigate this problem through a technique that selects numbers minimizing the occurrence of patterns ("pattern-free").

The technique is inspired by so-called Costas arrays (Costas, 1965; Golomb and Taylor, 1984; Drakakis and Rickard, 2010). A Costas array is a permutation of the unit matrix so that there is no equal distance between two nonzero elements. Thus, a shift creates, at most, a coincidence of two such elements.

Unfortunately, the construction of Costas arrays presents practical difficulties. First, Costas arrays of the dimensions 32 and 33 are not known in the literature. In addition, the definition of a Costas array does not lead to a simple method to find them. The only known way to find all Costas arrays for a given order is an exhaustive search. However, the number of Costas arrays of order N increases only up to a maximum of 21,104 for $N = 16$. After this order, the number drops quickly. Beard et al. (2004) show that there are only 200 Costas arrays of order 24. Exhaustive search, through the sequential generation of all $N!$ permutation matrices and checking the Costas condition, is prohibitively slow for large N.

For these reasons, we opted for a process inspired by one of the algorithms for finding Costas arrays for some dimensions, the so-called Welch algorithm (Golomb and Taylor, 1984). In our modification of this algorithm, for a total number N of shots in the survey, we first seek the smallest prime P greater than N. We then look for the largest prime T less than P that generates a complete permutation of the numbers from 1 to N by the following process. First, we calculate the sequence $n_j = T^j \mod P$, where n_j $(j = 1, \ldots, P)$ form a permutation of the numbers from 1 to P. In this sequence, we eliminate the elements $n_j > N$. If redundancy of shots within the set of groups is desired, we change T to the largest prime less than T that allows the construction and repeat the process. The thus obtained permutation vector defines the sequence in which the shots are grouped. If we want to build groups of K shots, each set of K values of this vector defines a group.

Note that the probability for the array found with this process to be a Costas array decays with increasing N. However, this construction process actually has an advantage over the use of true Costas arrays. Because of the limited number of Costas arrays existing for large N, the exclusive use of these arrays could lead to repeated groups in the case of shot redundancy.

A posteriori crosstalk reduction

Since it is impossible to prevent the occurrence of crosstalk when shot groups are migrated, another option is to remove it (or part thereof) after migration. Assuming that the noise is random and zero mean, we can apply existing techniques for removing such noise. In this study, we have tested the application of the nonlocal means (NLM) technique borrowed from image processing (Buadès et al., 2005, 2010; Bonar and Sacchi, 2012) and first applied to a seismic problem by Bonar and Sacchi (2012).

The NLM algorithm is a random-noise attenuation filter supposing that every image has a certain degree of redundancy, which can be used to highlight structures. The process searches, for each image point, other points whose neighborhoods are similar to the neighborhood of the original point, and uses these similarities to recover the image in this region. The fundamental process of the algorithm is an average over the whole image, applied with a weight that is determined by the similarities between the image in the vicinities under consideration.

Mathematically, the filtered image $\mathcal{I}$ is calculated from the original imagem I by the weighted average

$$\mathcal{I}(\mathbf{x}) = \sum_{\mathbf{x}'} \mathcal{W}(\mathbf{x}, \mathbf{x}') I(\mathbf{x}') \; , \quad (6)$$

where $\mathcal{W}(\mathbf{x}, \mathbf{x}')$ denotes the filter weights, calculated as

$$\mathcal{W}(\mathbf{x}, \mathbf{x}') = \frac{1}{Z(\mathbf{x})} \exp\left\{ \frac{-D^2(\mathbf{x}, \mathbf{x}')}{h^2} \right\} \; . \quad (7)$$

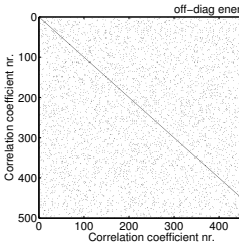

Figure 1: No shot encoding, no redundancy, 50 groups of 95 shots (reference matrix).

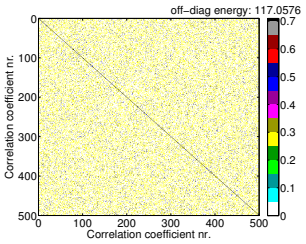

Figure 2: No shot encoding, redundancy with 50 groups of 380 shots.

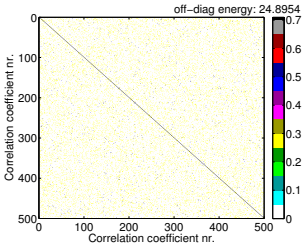

Figure 3: No shot encoding, redundancy with 200 groups of 95 shots.

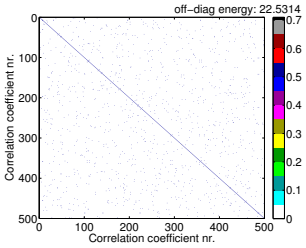

Figure 4: No shot encoding, no redundancy, 200 groups of 24 shots.

Here, h is a parameter that controls de exponential decrease and $Z(\mathbf{x})$ is a normalization factor, i.e.,

$$Z(\mathbf{x}) = \sum_{\mathbf{x}'} \exp\left\{\frac{-D^2(\mathbf{x},\mathbf{x}')}{h^2}\right\} . \qquad (8)$$

Function $D(\mathbf{x},\mathbf{x}')$ is a similarity measure between the vicinities of image points $\mathbf{x}$ and $\mathbf{x}'$. It is calculated as

$$D^2(\mathbf{x},\mathbf{x}') = \sum_{\mathbf{d}} G_a(d)\left[I(\mathbf{x}+\mathbf{d}) - I(\mathbf{x}'+\mathbf{d})\right]^2 , \qquad (9)$$

where $\mathbf{d}$ represents a dislocation vector of size d and function $G_a(d) = \exp(-d^2/a^2)$ represents a Gaussian window in which the parameter a defines the effective size of the neighborhood.

Numerical results

Weight matrix

To estimate the reduction in crosstalk in the migrated image achieved by the weights (2) to (5), we evaluate the matrices $\mathbf{W}$ generated by the product (1) of the weights and their proximity to the identity matrix. An important number in this sense is the energy ratio between the off-diagonal and diagonal of matrix $\mathbf{W}$. The lower this number, the better $\mathbf{W}$ approximates the Kronecker delta.

For our tests, we have used various groupings of a total of 4750 shots. If not mentioned otherwise, the comparisons are done with 50 groups of 95 shots each, i.e., no redundancy of shots. For a better visualization, the figures represent only the first 500×500 array elements. The number in the upper left corner of each figure is the ratio bewteen the off-diagonal and diagonal energy of the matrix, for simplicity from now on referred to as "energy factor". Note that for groups of K shots, without encoding the energy factor always takes the value $K-1$.

No encoding. Figure 1 shows the matrix $\mathbf{W}$ without shot encoding, i.e., for unit weights, $w_{gk} = \tilde{w}_{gk} = 1$. The choice

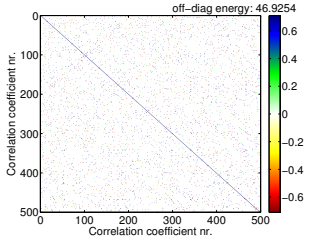

Figure 5: Continuous random phase encoding.

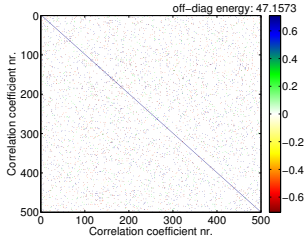

Figure 6: Random phase encoding, da fase, 16 levels.

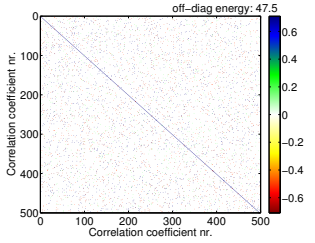

Figure 7: Random phase encoding, 10 levels.

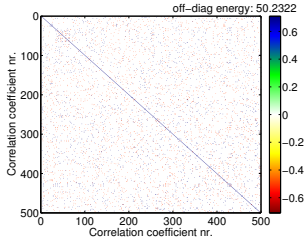

Figure 8: Random phase encoding, fase, 4 levels.

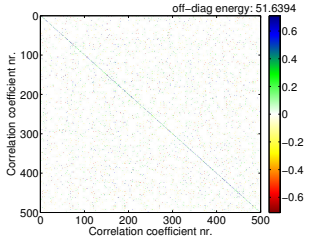

Figure 9: Continuous random amplitude encoding.

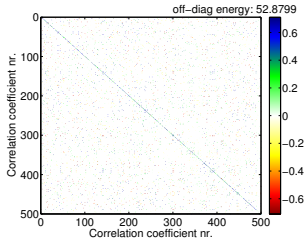

Figure 10: Random amplitude encoding, 16 levels.

of used sources was made randomly. We note that in this case the off-diagonal energy is 94 times greater than the diagonal energy, corresponding to 95 shots per group, as expected. When increasing the number of shots per group by a factor of four, to 380, the energy factor increases to 117 (Figure 2). Also, when maintaining 95 shots per group and increasing the number of groups to 200, to achieve the same fourfold redundancy, the energy factor reduced to approximately 25 (Figure 3). However, with 24 shots in each of the 200 groups, the energy factor decreased more strongly, to about 22 (Figure 4). Thus, for a given number of groups, one should use a minimum of sources per group. The use of shot redundancy is counterproductive.

Random phase encoding. The next set of figures shows the weight matrices for random phase encoding, for some possible levels of phase shift according to equation (2), for the case of 50 gropus of 95 shots. In Figure 5, we see the result of continuous phase eoncoding, i.e., allowing for all values between $-\pi$ and π. Figures 6, 7, and 8 show the corresponding results for 16, 10, and 4 levels, respectively. We observe that the continuous distribution yields the strongest reduction of the energy factor.

Random amplitude encoding. Figures 9, 10, 11 and 12 show the corresponding results for random amplitude encoding, with continuous distribution and 16, 10 and 4 levels. Again, we observe an increase in energy factor for a decreasing number of levels. In addition, we note that the magnitude of the diagonal is reduced (colored dots on the diagonal, where black indicates a unitary value). This

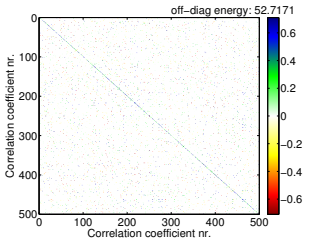

Figure 11: Random amplitude encoding, 10 levels.

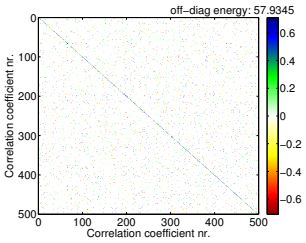

Figure 12: Random amplitude encoding, 4 levels.

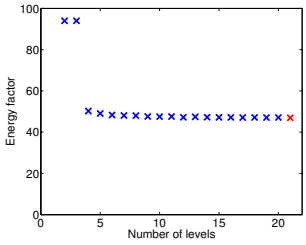

Figure 13: Energy factor as a function of level number for random phase encoding.

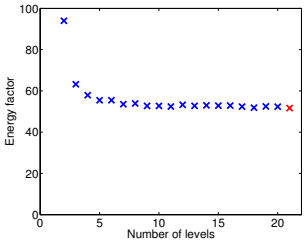

Figure 14: Energy factor vs. level number for random amplitude encoding.

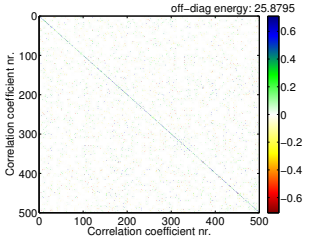

Figure 15: Continuous random phase and amplitude encoding.

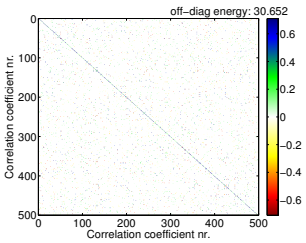

Figure 16: Random phase and amplitude encoding, 4 levels.

reduction is due to the fact that the product of the weights is not unitary, as mentioned in the context of equation (3).

The fact that the energy factors decreases for a growing number of levels, both for random phase and amplitude encoding, is corroborated in Figures 13 and 14, which show the energy factor as a function of the number of levels. We see that in both cases, the factor decays with increasing number of levels. We tested up to a maximum of 20 levels. The red dot at the end of the curve represents the continuous distribution.

Random phase and amplitude encoding. When we apply random encoding of both amplitude and phase, we obtain the matrices shown in Figures 15 and 16. We note that the simultaneous encoding further reduces the power factor, while the diagonal values are comparable with those for random amplitude encoding only. The decay of the energy factor with the number of levels is comparable to previous cases.

To avoid loss of information due to the reduction of the diagonal values, we also tested the effect of redundancy for this type of encoding. Figure 17 shows the weight matrix for 50 groups of 380 shots and Figure 18 shows the weight matrix for 200 groups of 95 shots. We observe the same effect as in the case without encoding, i.e., the energy factor increases with respect to the same number of groups without redundancy.

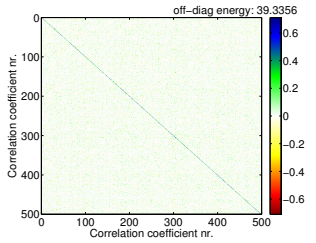

Figure 17: Continuous random phase and amplitude encoding, 50 groups of 380 shots.

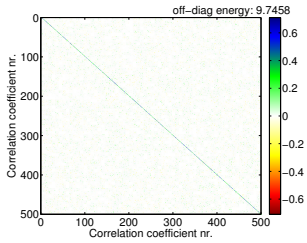

Figure 18: Continuous random phase and amplitude encoding, 200 groups of 95 shots.

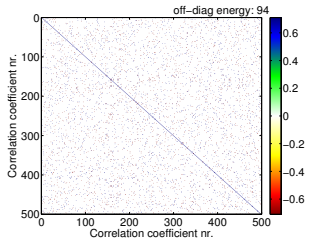

Figure 19: Random-sign encoding.

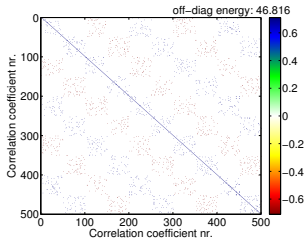

Figure 20: Imaginary-unit encoding.

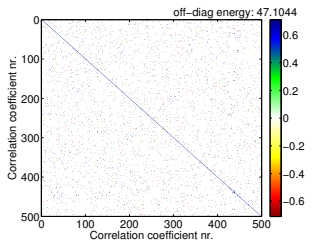

Figure 21: Random phase encoding combined with imaginary-unit weighting.

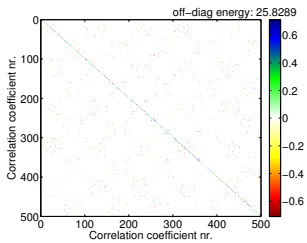

Figure 22: Random amplitude encoding plus imaginary-unit weighting.

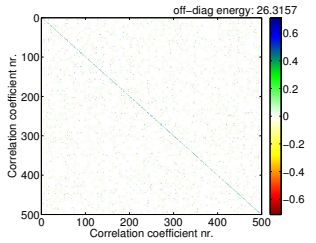

Figure 23: Random phase and amplitude encoding combined with imaginary-unit weighting.

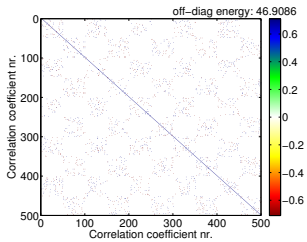

Figure 24: Random sign encoding combined with imaginary-unit weighting.

Random-sign and imaginary-unit encoding. Figure 19 shows the result of random sign encoding, equation (4). This encoding does not reduce the energy factor at all. Encoding with the imaginary unit, according to equation (5), reduces this factor by half (Figure 20) by transferring half the crosstalk to the imaginary part of the image.

Combinations. Finally, we investigate the combination of the imaginary-unit weight with random signal, amplitude and/or phase encoding. We note that the combination with random phase encoding does not achieve a further reduction of the energy factor (Figure 21). The reason is that random phase encoding already transfers energy to the imaginary part of the image, thus not offering the potential for a further reduction. On the other hand,

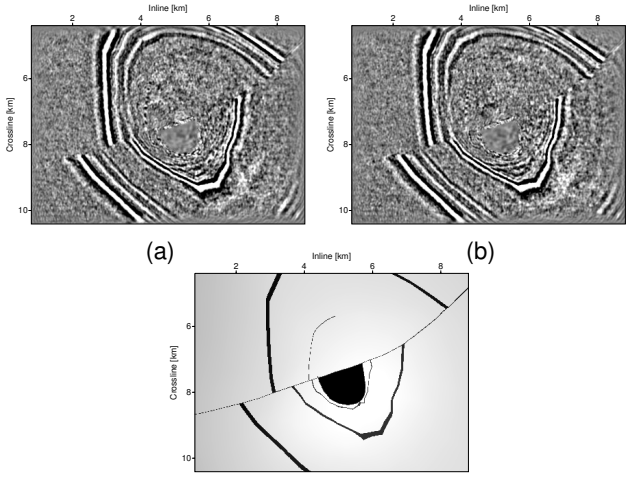

Figure 25: 3D FD migrated data from the SEG/EAGE salt model, depth slice at depth 680 m, with (a) random and (b) pattern-minimizing shot selection; (c) model slice.

the combination with random amplitude encoding reduces the energy factor significantly (Figure 22), reaching the same level as simultaneous random amplitude and phase encoding. The combination with random phase and amplitude encoding does not achieve a further reduction of the energy factor (Figure 23). Finally, the combination of imaginary-unit weighting with random sign encoding reduces the energy factor only to the same level achieved by imaginary-unit weighting alone (Figure 24).

3D migration tests

We tested random and pattern-minimizing shot selections in blended-shot migration using random phase encoding, applied to narrow azimuth data from the SEG/EAGE salt model with 4750 shots. To enhance the effect of crosstalk, migration was performed with a redundancy of 10, using 100 groups with 475 shots.

The following figures show depth slices at some selected depths. To our perception, at some depths the slices using pattern-minimizing shot selection are of better quality than those using random shot selection. At all other depths, the quality is comparable. This is the expected behavior, since the pattern minimization is supposed to reduce the probability for correlated shots to appear in the same group.

Figure 25 compares the depth slices at depth 680 m. The events are clearer in part (b), particularly those close to the salt body in the center of the image. At 1040 m depth (Figure 26), we observe a slight improvement in the definition of the right flank of the salt in Figure 26b.

However, not all parts of the image are visibly better with pattern-minimizing shot selection. While the salt in Figure 27b is still easier to delineate, particularly in the lower part of the image, the shape of the inclusion on the right side of the image is better represented in Figure 27a.

Our last figure is a slice from below the salt, at depth 2340 m (Figure 28). At this depth, the energy of the events is already significantly reduced by illumination effects. Still, the events in part (b) are generally more continuous and less rugged than in part (a).

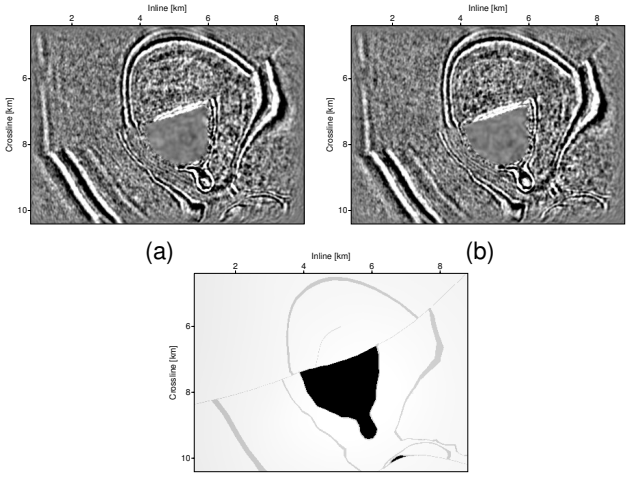

Figure 26: 3D FD migrated data from the SEG/EAGE salt model, depth slice at depth 1040 m, with (a) random and (b) pattern-minimizing shot selection; (c) model slice.

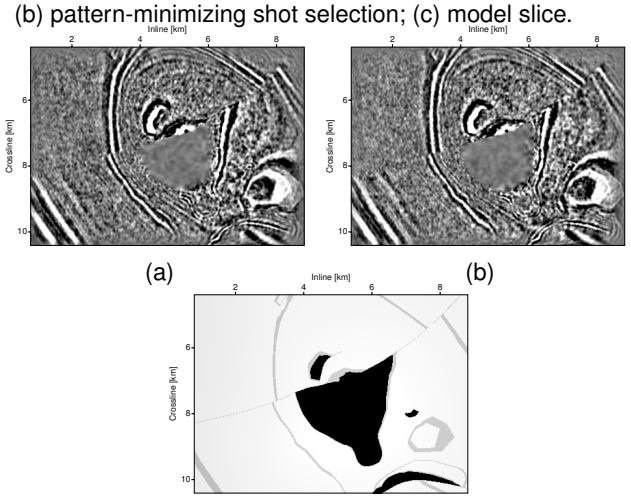

Figure 27: 3D FD migrated data from the SEG/EAGE salt model, depth slice at depth 1260 m, with (a) random and (b) pattern-minimizing shot selection; (c) model slice.

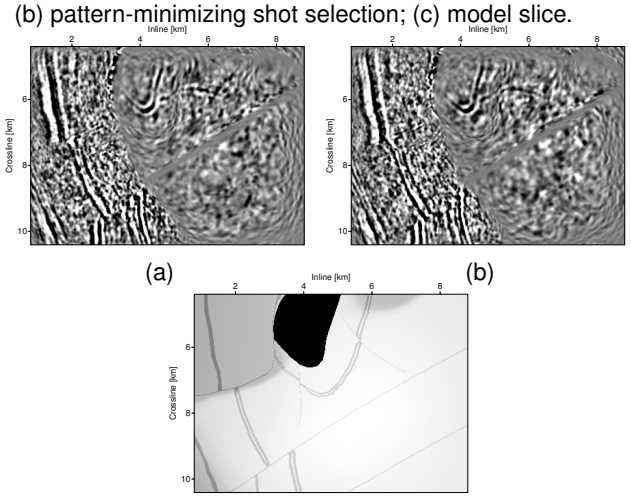

Figure 28: 3D FD migrated data from the SEG/EAGE salt model, depth slice at depth 2340 m, with (a) random and (b) pattern-minimizing shot selection; (c) model slice.

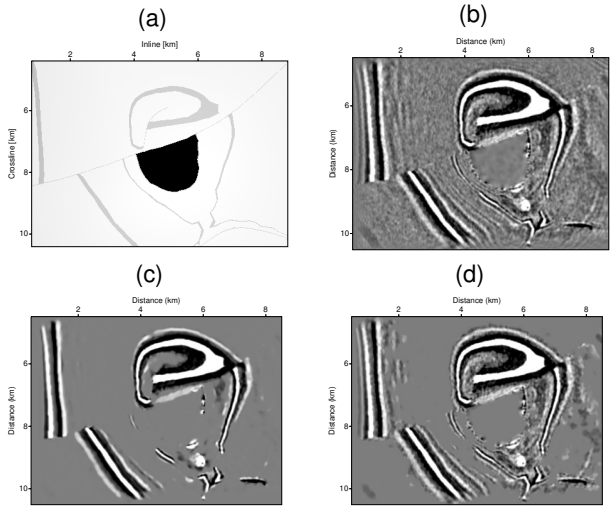

Figure 29: Depth slice at 1040 m depth of (a) SEG/EAGE salt model; and of the FD migrated section (b) without noise reduction and with NLM noise reduction with (c) $h = 10^{-4}$ and (d) $h = 1.5 \cdot 10^{-4}$.

A posteriori crosstalk reduction

To test the post-migration crosstalk reduction, we have implemented a 2D version of the nonlocal-means (NLM) algorithm following the original prescription of Buadès et al. (2005). Figure 29 compares the results at 1040 m depth with the original depth slice. The results strongly depend on the value of parameter h in equation (7). For smaller h, the processing can remove almost all noise caused by cross-talk, but some less energetic events are also attenuated (Figure 29c). In our tests, the characteristics of the result did not change as a function of depth. This result demonstrates that it is possible to mitigate crosstalk using image processing methods.

Conclusions

In this work, we studied possibilities of reducing crosstalk in blended-shot migration. In the first part, we evaluated the weight matrix of different encoding techniques.

In these tests, we found that for the investigated encoding methods, there is no advantage in admitting redundancy in the number of shots used. The choice of the number of shots per group should be always the ratio between the total number of shots and the number of groups to be realized. The fewer shots there are in each group, the lower is the off-diagonal energy in the weight matrix. This conclusion, however, needs to be confirmed in actual migration tests, since destructive interference might help to further reduce crosstalk, even if the content of off-diagonal energy is higher. Also, random amplitude encoding helps to improve the ratio between the energy on and off the diagonal. Although this encoding reduces the energy contained in diagonal, it reduces the off-diagonal energy more strongly, so that the amplitude of the crosstalk declines more than the amplitude of the image.

Random phase encoding contributes to the reduction of crosstalk mainly by the fact that part of the off-diagonal energy is transferred to the imaginary part of the image. This effect is exploited to the maximum by applying a deterministic imaginary-unit weight, which moves every second term of the crosstalk to the imaginary part. The strongest reduction of off-diagonal energy in the weight matrix was achieved by combining this weight with random amplitude encoding. In our tests, this reduced crosstalk to approximately a quarter of its nominal value.

In addition to this evaluation of the encoding weights, we studied how to select the shots to form groups to be migrated. Comparing a random-selection method with another one designed to minimize patterns, we observed a trend of the latter to provide clearer, more easily delineated events in the image.

Finally, we investigated the possibility of reducing the noise generated by crosstalk in a processing step applied after migration by means of the nonlocal-means method. In our tests, the noise behaved favorably to this method, so that it was possible to remove much of the crosstalk. This result demonstrates that it is possible to mitigate the crosstalk noise by image processing methods.

Acknowledgments

This work was kindly supported by CNPq as well as Petrobras and the sponsors of the Wave Inversion Technology (WIT) Consortium.

References

Beard, J. K., J. C. Russo, K. Erickson, M. Monteleone, and M. Wright, 2004, Combinatoric collaboration on costas arrays and radar applications: IEEE National Radar Conference - Proceedings, 260–265.

Bonar, D., and M. Sacchi, 2012, Denoising seismic data using the nonlocal means algorithm: Geophysics, **77**, A5–A8.

Buadès, A., B. Coll, and J. M. Morel, 2005, A review of image denoising algorithms, with a new one: Multiscale Modeling and Simulation, **4**, 490–530.

———, 2010, Image denoising methods. a new nonlocal principle: SIAM Review, **52**, 113–147.

Costas, J. P., 1965, Medium constraints on sonar design and performance: Class1 Report R65EMH33, G.E. Corp.

Drakakis, K., and S. Rickard, 2010, On the construction of nearly optimal golomb rulers by unwrapping Costas arrays: Contemp. Engineering Sciences, **3**, 295–309.

Godwin, J., and P. Sava, 2010, Blended source imaging by amplitude encoding: SEG Exp. Abstracts, 3125–3129.

———, 2011, A comparison of shot-encoding schemes for wave-equation migration: SEG Exp. Abstracts, 32–36.

Golomb, S. W., and H. Taylor, 1984, Constructions and properties of Costas arrays.: Proceedings of the IEEE, **72**, 1143–1163.

Guerra, C., and B. Biondi, 2008, Phase encoding with gold codes for wave-equation migration: SEP Report, **136**, 23–42.

Romero, L. A., D. C. Ghiglia, C. C. Ober, and S. A. Morton, 2000, Phase encoding of shot records in prestack migration: Geophysics, **65**, 426–436.

Soubaras, R., 2006, Modulated-shot migration: SEG Exp. Abstracts, SEG, 2430–2434.

Sun, P., S. Zhang, and F. Liu, 2002, Prestack migration of areal shot records with phase encoding: SEG Exp. Abstracts, SEG, 1031–1034.

Temme, P., 1984, A comparison of common-midpoint, single-shot, and plane-wave depth migration: Geophysics, **49**, 1896–1907.